

Comparative binding efficacy of Ivermectin and Remdesivir against the spike protein of Omicron variants: An *in silico* perspective

Ritwik Patra¹, Parth Sarthi Sen Gupta², Saroj Kumar Panda³, Malay Kumar Rana³ & Suprabhat Mukherjee^{1*}

¹Integrative Biochemistry & Immunology Laboratory, Department of Animal Science, Kazi Nazrul University, Asansol-713 340, West Bengal, India

²School of Biosciences & Bioengineering, D. Y. Patil International University, Akurdi, Pune-411 044, Maharashtra, India

³Department of Chemistry, Indian Institute of Science Education and Research, Berhampur-760 010, Odisha, India

Received 19 February 2024; revised 26 August 2025

The recent emergence of SARS-CoV-2 Omicron variants (B.1.1.529) has come out as an added complication in combating COVID-19. Different repurposed drugs like ivermectin, hydroxychloroquine, remdesivir, molnupiravir are being investigated to treat these variants. Herein, we investigate the comparative binding efficacy of ivermectin, remdesivir, hydroxychloroquine, favipiravir, paxlovid, and molnupiravir against the mutant spike protein of omicron variants. Molecular docking data revealed that ivermectin ($\Delta G = -430.56$) and remdesivir ($\Delta G = -352.78$) exhibit the higher binding efficacy to the spike protein mutants (N501Y, Q493R, Q498R, S373P, S375F, T478K, S371L, H655Y, N679K, P681H) of the Omicron variants, wild type SARS-CoV-2 and a hypothetical spike protein bearing all the mutations. Normal mode analysis and molecular dynamic simulation hinted at the stability of binding of ivermectin and remdesivir to spike protein mutant (T478K) compared to the less active drugs. This study highlights the significance of computational methods in enhancing drug discovery and repurposing through expedited analyses of molecular interactions, stability, and binding efficacy. It serves as an essential preliminary phase in pinpointing the potential therapeutic candidates for subsequent validation via *in-vitro* and *in-vivo* investigations. Collectively, this *in silico* study proposed that ivermectin and remdesivir could serve as promising therapeutics in intervening with the omicron variants.

Keywords: Corona Virus, Ivermectin, Molecular docking, Omicron, SARS-CoV-2

The worldwide COVID-19 pandemic, originating in the Chinese province of Wuhan has exacted a heavy toll on humanity. As of the end of January 2024, more than 774.291 million confirmed cases and 7.019 million deaths have been reported globally¹. Despite the development of various therapeutic measures, the emergence of different variants has presented challenges. The considerable genome size of SARS-CoV-2 (~30 kb) coupled with the low fidelity of its replication machinery serves as a prime factor for the virus's adaptation through mutations within the host². From January 2021 onwards, the World Health Organization (WHO) has identified Alpha, Beta, Gamma, and Delta as the principal variants of concern (VOCs), which have been associated with increased transmission rates and immune escape mechanisms¹⁻³. In November 2021, the Omicron variant B.1.1.529 was first detected and classified by WHO as the

variant with the highest number of mutations. The mutation frequency of Omicron has led to this variant becoming highly contagious, spreading to over 188 nations within four months^{2,4}.

The coronavirus possesses an unsegmented, positive-sense RNA genome measuring approximately 30kb, combined with glycoproteins-enriched surface proteins such as the spike, membrane, and envelope. It encodes for four structural proteins — the membrane glycoprotein (M), nucleocapsid (N), envelope (E), and spike protein (S) — in addition to several nonstructural proteins (NSPs)^{3,4}. NSPs are inclusive of the main protease (Mpro), RNA-dependent RNA polymerase (RdRp), and nine accessory proteins (Orf3a, Orf3b, Orf6, Orf7a, Orf7b, Orf8, Orf9b, Orf9c, and Orf10)^{3,4}. The spike protein acts as a crucial factor in the immunopathogenesis of coronavirus disease. Comprising two subunits, S1 and S2, and furin protease cleavage sites, the S1 subunit contains the N-terminal domain (NTD) and the receptor-binding domain (RBD). The binding of the viral spike protein to the human angiotensin-converting enzyme 2 (ACE2) and the support of another human protein, TMPRSS2, mediates

*Correspondence:

E-mail: suprabhat.mukherjee@knu.ac.in

Suppl. data available on respective page of NOPR

the interaction between the virus and the host⁵⁻⁷. Notably, the Omicron variant's spike glycoprotein harbours numerous mutations, including 28 amino acid substitutions, three deletions, and one insertion (A67V, Δ69-70, T95I, G142D, Δ143-145, Δ211, L212I, ins214EPE, G339D, S371 L, S373P, S375F, K417N, N440K, G446S, S477N, T478K, E484A, Q493R, G496S, Q498R, N501Y, Y505H, T547K, D614G, H655Y, N679K, P681H, N764K, D796Y, N856K, Q954H, N969K, L981F), 15 of which are situated within the RBD.² Mutations in RBD are present in all Omicron clades, contributing to viral survivability, infectivity, and evasion of immune responses. Prior research has indicated that mutations including H655Y, N679K, and P681H stimulate furin protease-mediated cleavage of S1/S2, facilitating virus-human cell membrane fusion, heightening replication and infectiousness of the Omicron variant of SARS-CoV-2^{8,9}. Moreover, Omicron variant heightens the risk of COVID-19 reinfection. The interactions between viral antigens and host immune cells are crucial in defining the disease's immunopathological features. The resulting proinflammatory reactions, such as vasodilation and humoral component accumulation, affect the clinical outcomes¹⁰⁻¹². Vasodilation and the accumulation of humoral components caused by proinflammatory responses brought on by host-virus interactions lead to the result.

Recent studies in this direction have leveraged computational approaches to identify potential drug repurposing candidates for SARS-CoV-2^{10,13-19}. Molecular docking and dynamics simulations have been extensively employed to assess the binding affinity of the existing drugs to the spike protein of the virus. Machine learning techniques have also been explored to predict drug-target interactions and prioritize potential repurposing candidates^{7,20}. Moreover, a couple of studies have also validated the effectiveness of SARS-CoV-2 prophylaxis using the antimalarial drug hydroxychloroquine in tandem with the antibacterial azithromycin and antiretroviral drugs including remdesivir, EIDD-2801, and favipiravir^{18,19}. Moreover, in-vitro research on U.S. FDA-approved drugs has demonstrated ivermectin to be notably potent against COVID-19²¹. Nevertheless, the variations of SARS-CoV-2 have led to disparities in virulence, transmissibility, reinfection rates, disease severity, and immune responses, including vaccines' ability to confer immunity or potential evasion by the pathogen. To address the knowledge gaps regarding the efficacy of repurposed drugs against SARS-CoV-2 Omicron variants, this study employs *in silico* methods

to compare the binding affinities of ivermectin, remdesivir, hydroxychloroquine, favipiravir, paxlovid, and molnupiravir to the spike protein. Molecular docking, normal mode analysis, and molecular dynamics simulations are utilized to investigate the interactions between these drugs and the Omicron spike protein mutants. The aim is to assess the potential of these repurposed drugs as effective therapeutics by evaluating their direct binding ability to inhibit the spike protein interactions crucial for viral entry and immunopathogenesis. This study will provide valuable insights into the stability and efficacy of these drugs, potentially guiding future experimental and clinical research efforts — against the most virulent Omicron variants of SARS-CoV-2, employing advanced bioinformatic approaches.

Material and Methods

Data mining

The GISAID database (<https://www.gisaid.org/>) was explored to collect data regarding the various mutations on the spike glycoprotein of the Omicron variant (B.1.1529)²². The native wild-type spike glycoprotein (Accession ID: QHD43416.1) of SARS-CoV-2 was obtained from the NCBI database (<https://www.ncbi.nlm.nih.gov/>) and was used to generate the model for the different mutant variants²². Moreover, a single model was generated containing all the different mutations of spike glycoprotein. The different drugs used in this study include ivermectin B1a (compound CID: 6321424), ivermectin B1b (compound CID: 6321425), remdesivir (compound CID: 121304016), hydroxychloroquine (compound CID: 3652), favipiravir (compound CID: 492405), paxlovid (compound CID: 155903259), molnupiravir (compound CID: 14 5996610) used were obtained from PubChem library (<https://pubchem.ncbi.nlm.nih.gov/>). The commercially used ivermectin consisting of a racemic mixture of 5-O-demethyl-22,23-dihydroavermectin B1a (ivermectinB1a) and 5-O-demethyl-25-de(1-methylpropyl)-22,23-dihydroavermectin B1b (ivermectin B1b) and herein this study we used both the structures²¹. The structures were converted into 3D conformers followed by .pdb format with minimal energy²¹.

Homology modeling and validation

Homology modeling was executed for the spike proteins of Omicron variants with single mutant amino acids and for BA.1, BA.2, BA.2.12.1, BA.4,

and BA.5 Omicron groups. Later, a unique spike protein structure was modeled, utilizing all the mutant amino acids responsible for all Omicron co-variants. All the experiments to achieve the models of the mutant form were accomplished by utilizing a fully automated template-based SwissModel web tool (<https://swissmodel.expasy.org/interactive>). Later to validate the stereochemical nature of the 3D structure of each mutant Omicron spike protein and monoclonal antibodies SAVES (<https://saves.mbi.ucla.edu/>) server was utilized with different parameters *viz.*, ERRAT, VERIFY 3D, PROVE AND PROCHECK^{14,21}.

Molecular docking and visualization

The interaction of the validated structures of the omicron spike proteins with the drugs was studied using Hex 8.0.0 software package (<http://hexserver.loria.fr/>), which is an FFT (Fourier transform)- based docking server for protein^{21,23}. In Hex 8.0.0, a standard 6D docking run took ~15 seconds utilizing two graphics processors concurrently. The PDB file of the spike proteins was given as receptors and the six drugs were used as ligands for analyzing the interactions between them based on different parameters such as shape plus electrostatic correlations²³. After completion of the docking process, E total-values (Energy values) of each docked complex were recorded for further study (Table S1). The interactions of the docked complexes were then visualized using Discovery Studio 2021 Client software.

Determination of molecular interactions

From the docking result, we have screened the drugs that have a docking score of < -100 with the different structures of omicron variants. Thereafter, we determined the top 10 most virulent mutations of the omicron variant and selected them for studying the different types of molecular interactions within docked complexes. Molecular interactions between the docked complexes were determined by using a Python-based Protein-Ligand Interaction Profiler (PLIP) server (<https://projects.biotec.tu-dresden.de/>). PLIP follows the rule-based algorithm, for detection and visualization of non-covalent protein-ligand bonds.²⁴ This server could detect seven types of interactions in the docked complexes such as hydrogen bonds, hydrophobic interactions, salt bridges, water bridges, halogen bonds, π -cations interactions, π - stacking²¹.

Normal Mode Analysis (NMA)

After observing the interactions study investigation of the molecular flexibility of the docked structures was done using the WEBnma v2.0 server (<http://apps.cbu.uib.no/webnma>). The online server compares the dynamics of all proteins in the provided set sequentially by implementing two metrics: the Root Mean Squared Inner Product and the Bhattacharyya Coefficient²⁵. PDB format of the docked structures were submitted to this server to compute atomic fluctuations, deformations, correlation matrix plots, and eigenvalues that showed the dynamics and flexibility. Eigenvalue and atomic deformation frequency confirmed the rigid and non-rigid parts of the complexes²⁶. Moreover, using this online server the dynamics of the molecules of the complex structures were also determined.

Molecular dynamics simulation analysis

The stability of protein-ligand complexes can be investigated using MD simulations, which also aid in revealing the atomic details of the complexes that cannot be observed experimentally. Here, we have used Gromacs2022 to perform 50 ns MD simulations of the different selected docked structures²⁶⁻²⁸. Proteins were initially energy-minimized using the Amber99sb force field²⁹. Antechamber in ACPYPE was used to create the small molecule topology. In a cubical box with 10Å edges size, the systems are solvated. Using a concentration of 0.15 mol/L NaCl, the entire system was electrically neutralized. All complexes underwent a 5000-step steepest descent integrator energy minimization process. Following that, the systems were equilibrated for 5 ns each using the NVT and NPT ensembles. Each system was connected to a temperature controller (Berendsen) and a pressure controller (Parrinello-Rahman) to keep the temperature at 300 K and the pressure at 1 bar. Particle mesh Ewald (PME) technology with a 0.12 nm Fourier grid spacing was used to calculate the long-range Coulomb interactions. Using a cut-off distance of 1 nm, the Lennard-Jones potential was used to simulate the short-range van der Waals interactions. All bond lengths were constrained using the linear constraint solver (LINCS) method. The final MD simulations for the equilibrated structures were then ran for 50 ns. The trajectories of the systems were extracted for post-MD studies after the MD simulation was finished. All the post-MD analyses such as root-mean-square-deviation (RMSD), root-mean-square-fluctuation (RMSF), radius of gyration (Rg), hydrogen bond (H-bond), solvent accessible surface area (SASA),

principal component analyses (PCA), *etc.* were analyzed for all the complexes.

MM-PBSA binding free energy calculations

The binding free energy was calculated using the Molecular Mechanics Poisson Boltzmann Surface Area (MM-PBSA) method³⁰. The binding free energy is calculated as follows,

$$\Delta G_{Bind} = \Delta G_{complex} - (\Delta G_{protein} + \Delta G_{ligand})$$

The above equation can be divided into many interaction energies and can be expressed as,

$$\Delta G_{Bind} = \Delta H - T\Delta S = \Delta E_{MM} + \Delta G_{Sol} - T\Delta S$$

Where,

$$\begin{aligned} \Delta E_{MM} &= E_{bonded} + E_{non-bonded} \\ &= \Delta E_{int} + \Delta E_{vdW} + \Delta E_{elec} \end{aligned}$$

Where, E_{int} represents the total bonded interaction, which includes bond, angle, dihedral, and inappropriate interactions; and $E_{non-bonded}$ represents the total non-bonded interaction, which includes van der Waals (E_{vdw}) and electrostatic (E_{elec}) interactions. E_{int} is always assumed to be zero.

$$\Delta G_{sol} = \Delta G_{PB} + \Delta G_{SA}$$

Again,

$$\Delta G_{SA} = \gamma SASA + b$$

where γ (a coefficient related to the surface tension of a solvent) = 0.02267 kJ/mol/Å², and b = 3.849 kJ/mol.

Results and Discussion

Selection of the repurposed drugs

The highly mutated variant of SARS CoV-2, omicron is very infective and has a risk of reinfection. In this context, the COVID-19 vaccines failed to protect against this variant. However, from the limited information about omicron, we tried to find an efficacious drug for the management of this variant. To find the most efficient one we took the most common six multipurpose drugs for our investigation. We selected the most used repurposed drugs depending on different parameters such as mode of action, general usage, consumers' age group, *etc.* Among them, ivermectin is an antiparasitic medicine licensed by the Food and Drug Administration (FDA) that is used to treat a variety of neglected tropical diseases such as onchocerciasis, helminthiasis, and scabies. Besides, the parasiticidal action it is also been reported as an antiviral drug recently. On the other

hand, remdesivir was designed for use on new pathogenic RNA viruses in 2016 and was found to be effective on viral respiratory infections³¹. It restricted the viral RNA strand elongations at the time of replication and works as a viral RNA polymerase inhibitor³². Hydroxy-chloroquine is a well-known antimalarial drug, which is also used for the treatment of rheumatoid arthritis and systemic lupus erythematosus³³. Whereas, favipiravir is a repurposed drug, usually used in the treatment of viral infections such as influenza. During the SARS-CoV-2 pandemic, Wuhan first used it against COVID-19 infections³⁴. Both anti-viral drugs molnupiravir and paxlovid are FDA-approved for use against COVID-19 variants, but only paxlovid is authorized to be consumed by the age group below 18 years³⁵.

Molecular docking and molecular interaction of the spike proteins with the drugs

Our study intends to look into the interactions between the spike proteins and our selected drugs by performing molecular docking. In HEX docking, the primary metric for evaluating the binding affinity of molecular docking is the scoring function. This function assigns a numerical value to each pose based on factors such as intermolecular energy (*e.g.*, van der Waals forces, hydrogen bonds, electrostatics), solvation energy, and entropy and represented as Energy-value (E Total-value). A lower E Total-value score generally indicates a more favorable binding pose. In our study, we screened the docked complexes based on E Total-values, which were <-100. We eliminated the drug Favipiravir from our selected list of drugs as all the E- values of this drug were greater than -100, which indicates poor efficiency of binding to the spike proteins (Table S1, and Fig. 1). Later, we screened and selected the 10 most virulent omicron variants viz., N501Y, Q493R, Q498R, S373P, S375F, T478K, S371L, H655Y, N679K, P681H based on the previous literature that showed comparatively high efficiency of binding with the five different drugs, based on their E Total-values (Table 1).

Herein, we have selected the best docking result from each of the five drugs for analysing the different types of biomolecular interactions. The molecular docking of ivermectin with T478K ensures its role in inhibiting the entry of the virus into the host. Ivermectin increases the endosomal pH and inhibits the replications as well as the post-translational mechanism of viral glycoproteins³². On the other side remdesivir also shows higher binding affinity to

Table 2 — Comparative protein-ligand interactions amongst different drugs and omicron mutant structures based on the highest docking value

Name of Drug	Mutation	Docking Score (E Total)	Residue	Amino acid	Types of Interaction		
					Distance (in Å)	Ligand Atom No.	Protein Atom No.
Ivermectin B1a	T478K	-430.56	734A	THR	Hydrophobic interaction		
			2521C	PRO	2.35	32414	7054
					3.34	32427	24137
			734A	THR	Hydrogen bonding		
			2789C	ASN	2.30	3.25	178.41
					2.95	3.91	160.33
Ivermectin B1b	T478K	-339.37	2104B	LYS	Hydrophobic interaction		
					3.21	32401	20079
					Hydrogen bonding		
			39A	GLN	2.98	3.79	142.10
Remdesivir	H655Y	-352.78	2104B	LYS	3.05	3.98	149.02
			1422B	TYR	Hydrophobic interaction		
					3.90	32224	13664
			1416B	SER	Hydrogen bonding		
					3.20	4.01	143.95
					Hydrophobic interaction		
Hydroxychloroquine	H655Y	-1456.44	2983C	GLU	3.65	32208	28517
			3225C	GLU	3.84	32188	30776
			2983C	GLU	Hydrogen bonding		
			2986C	ASN	1.93	2.44	111.82
					3.06	3.79	131.18
					Salt Bridge		
Paxlovid	T478K	-251.67	1538B	ASP	4.20		
			1539B	ASP	4.77		
			836A	LEU	Hydrophobic interaction		
Molnupiravir	H655Y	-226.6	817A	ASP	3.29	32408	8030
					3.93	32407	7857
			940A	ASN	Hydrogen bonding		
				3.26	3.92	125.49	
			940A	ASN	3.73	4.01	100.28

while hydrogen bonds and hydrophobic interactions are significant, the binding energy offers a more holistic perspective on the strength and potential therapeutic efficacy^{37,38}. For instance, the strong binding affinity of ivermectin can be attributed to a combination of specific hydrogen bonding with key residues and robust hydrophobic interactions^{17,18,21}. This suggests a greater likelihood of the drug remaining bound to the spike protein under physiological conditions, potentially hindering viral entry or subsequent infection stages. However, competitive inhibition and potential off-target effects must be carefully evaluated. Although the high binding affinities of ivermectin and remdesivir suggest they could effectively compete with the virus's natural ligands, further in-vitro and in-vivo studies are necessary

to confirm their specificity and safety without interfering with critical host proteins.

Normal mode analysis (NMA)

NMA is a helpful tool for assessing the flexibility of two interacting proteins that exist as an assembly across multiple modes of the protein complex's structure¹⁴. The protein-protein interaction between the complexes shown by the correlation matrix plot in (Fig. 3iii) demonstrated connections of the residues of the docked complexes. The red color in the plot signified correlated, blue signified anti-correlated, and white signified uncorrelated motion of the complexes, and the direction of the motions within the complexes was shown by the arrows in the plot. Deformation

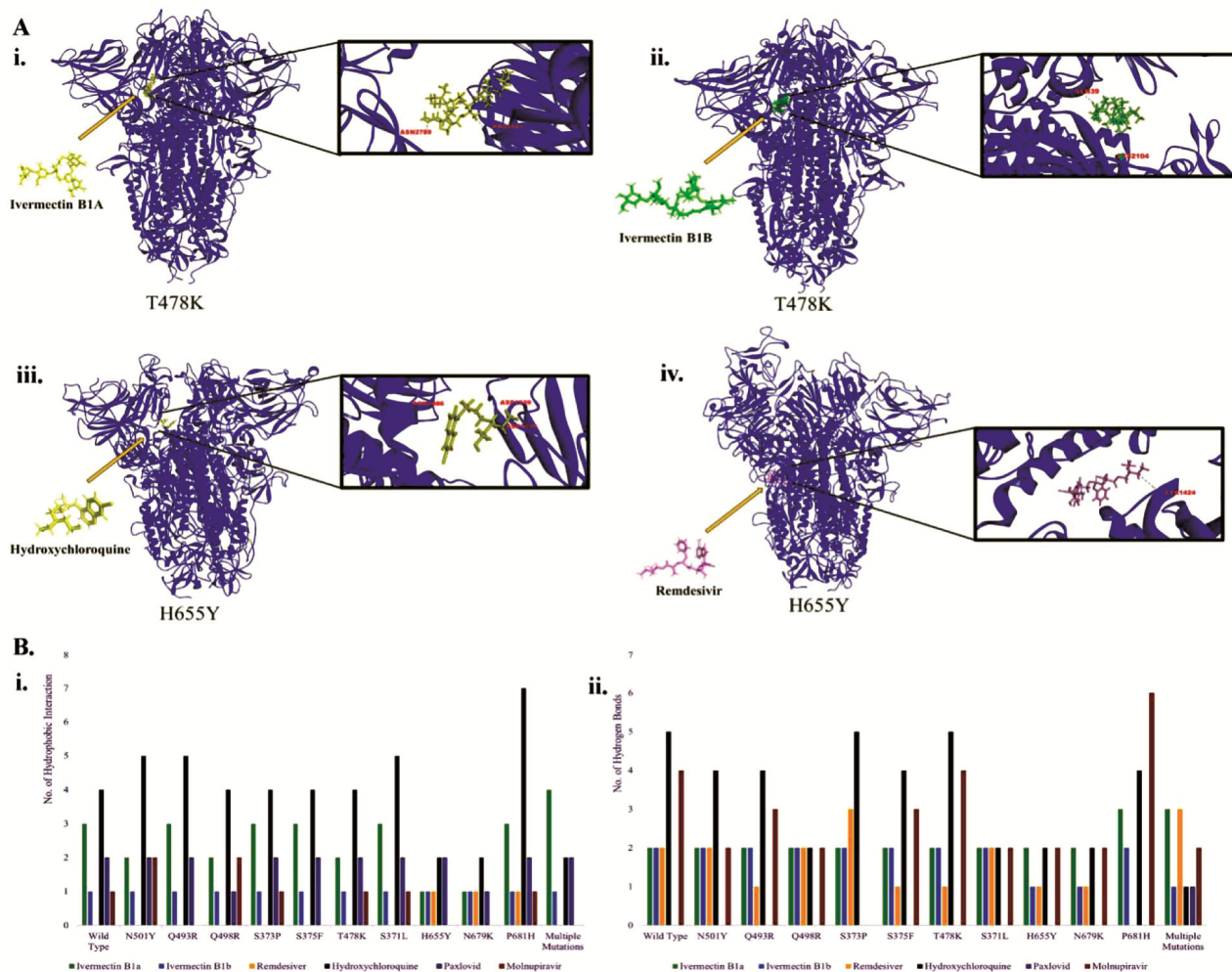


Fig. 2 — Interaction of screened drugs with mutant viral proteins; (A) Interacting residues of the docked complexes between screened drugs with viral proteins, i. Ivermectin B1a-T478K complex, ii. Ivermectin B1b-T478K complex, iii. Hydroxychloroquine-H655Y complex, iv. Remdesivir-H655Y complex; and (B) Comparative protein-ligand interactions amongst different drugs and omicron mutant structures; i. The number of hydrophobic interactions, ii. The number of hydrogen bonds

energy and eigenvalues are inversely proportionate to the amplitude motion. The associated energy level of each mode within the complexes was shown in (Table 3 and Figs. 3i and 3ii), through the deformation energy plot and eigenvalue plot. The atomic fluctuations and displacement of mode 7 are shown in (Fig. 4). Depending on the deformation energy, eigenvalue, displacement, fluctuation plot, and correlation matrix, numerous modes were constructed to forecast the stability of the docked structure (Fig. 3), our results show that the deformation energy of Ivermectin B1b is even less than its isotope B1a (Table 3). Moreover, these results suggested that the docked complex of ivermectin B1b-T478K resembles flexibility as well as stability.

Table 3 — Deformation energy of the docked complexes

Drugs	Mutant Structure	Deformation Energy
Ivermectin B1a	T478K	3.94
Ivermectin B1b	T478K	3.924
Remdesivir	H655Y	3.456
Hydroxychloroquine	H655Y	12.864
Paxlovid	T478K	3.924
Molnupiravir	H655Y	3.729

Molecular dynamics simulation (MDS) Study

The stability of the docked complexes was further validated using MDS trajectory analyses employing different force fields to examine the effect of the solvent on the interacting complexes and their types of physical interactions. Herein, the stability of the docking of the different drugs to the respective spike proteins was analyzed by evaluating the

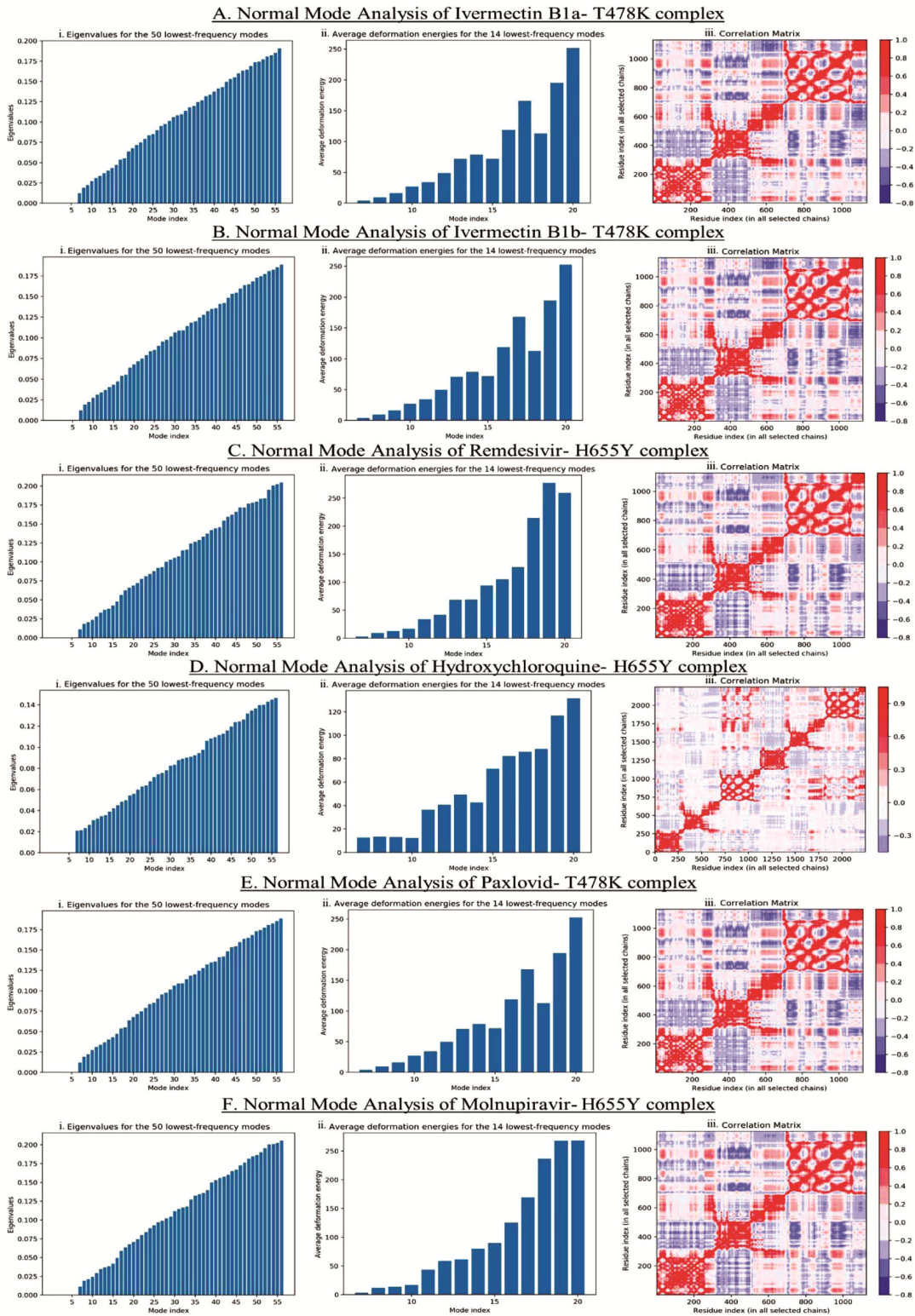


Fig. 3 — Normalmode analysis of the docked structures (A) Normal Mode Analysis of ivermectin B1a-T478K complex, (B) Normal Mode Analysis of ivermectin B1b-T478K complex, (C) Normal Mode Analysis of remdesivir-H655Y complex, (D) Normal Mode Analysis of H655Y+HCQ4 complex, (E) Normal Mode Analysis of paxlovid-T478K complex, and (F) Normal Mode Analysis of molnupiravir-H655Y complex representing i. Eigenvalues, ii. Average deformation energies of different modes, iii. correlation matrix

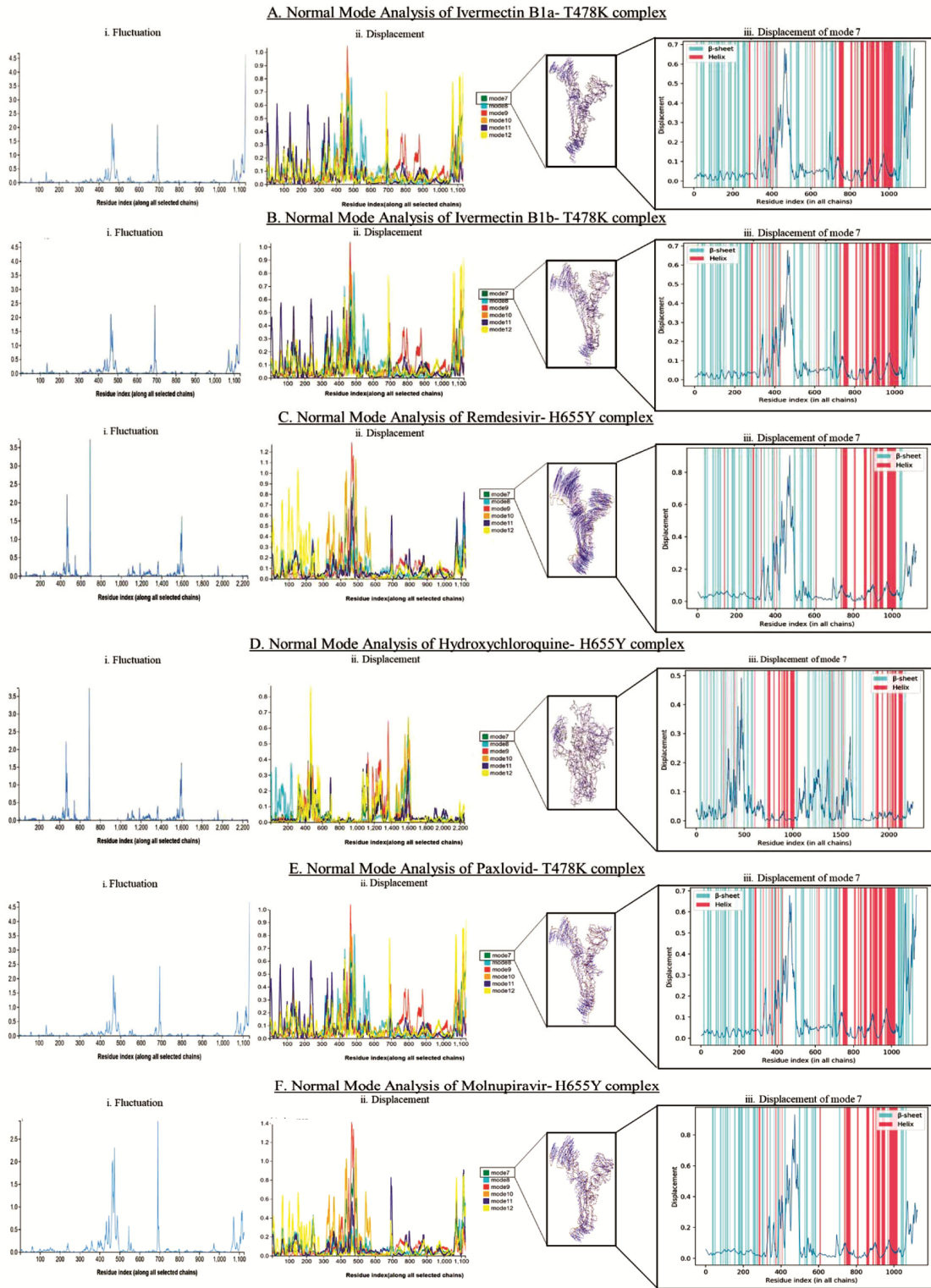


Fig. 4 — Comparative analysis of fluctuation and displacement between the docked complexes; (A) Normal Mode Analysis of ivermectin B1a-T478K complex; (B) Normal Mode Analysis of ivermectin B1b-T478K complex; (C) Normal Mode Analysis of remdesivir-H655Y complex; (D) Normal Mode Analysis of H655Y+HCQ4 complex; (E) Normal Mode Analysis of paxlovid-T478K complex; and (F) Normal Mode Analysis of molnupiravir-H655Y complex representing i. Fluctuation plot, ii. displacement plot, and iii. Displacement of the best mode (mode 7)

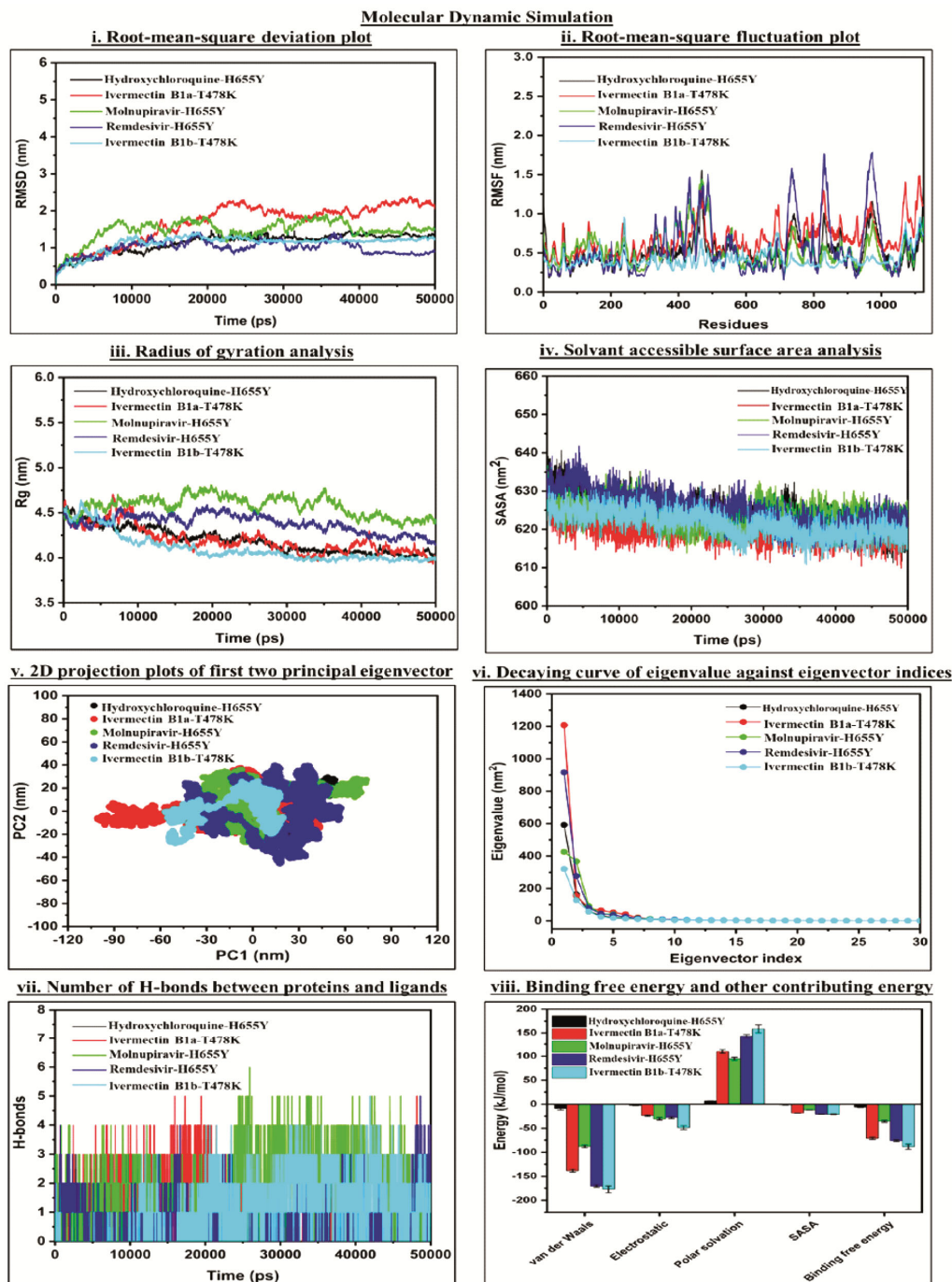


Fig. 5 — Molecular dynamic simulation study, the Hydroxychloroquine-H655Y complex represents in black, ivermectin B1a- T478K complex represents in red, molnupiravir-H655Y complex represents in green, remdesivir-H655Y complex represents in blue and ivermectin B1b-T478K complex represents in cyan. i. Root-mean-square-deviation, ii. Root-mean-square-fluctuation, iii. Radius of gyration analysis, iv. Solvent accessible surface area analysis v. 2D projection plots of first two principal eigenvectors, vi. The decaying curve of eigenvalue against eigenvector indices coming from covariance matrix, vii. Number of H-bonds between proteins and ligands, viii. Binding free energy and all the contributing energy (in kJ/mol)

root-mean square-deviation (RMSD), root-mean square-fluctuation (RMSF), radius of gyration (Rg), and solvent accessible surface area (SASA) plots within the definite MD trajectory (Fig. 5). The RMSD measures

the average distance that atoms deviate from their initial positions. Figure 5i shows that the RMSDs of all complexes are rather constant and smooth over the course of the simulation, however, some complexes,

like ivermectin B1a-T478K and molnupiravir-H655Y, exhibit more significant deviations. We have generated snapshots at 0 ns and 50 ns to gain a better understanding of the stability of all complexes and have found that except for hydroxychloroquine-H655Y, all of the protein-ligand complexes are stable across the whole dynamical time scale.

However, the RMSD of the hydroxychloroquine-H655Y complex is not stable. This is because the secondary structure of the spike protein is very stable. Some loop sections deviate across the simulation periods, although in most cases the RMSD remains quite consistent. Protein C α -atom variations are also monitored using RMSF during extended simulation times. The C α atoms of the remdesivir-H655Y complex were found to exhibit more fluctuations than any of the other atom types (Fig. 5ii). It was found that the loop areas of all the cases exhibit the same level of fluctuation. The compactness of proteins is quantified by Rg. Here it can be shown from Figure 5 that all the systems remain compact throughout the simulation times. SASA measures the solvent-accessible surface area of protein-ligand complexes. Instability increases as SASA increases. In this case, SASA values across all systems are extremely similar and tend to drop slowly over time (Fig. 5iv).

According to the MD snapshots (Suppl. Fig. S2), the hydroxychloroquine-H655Y system is unstable, with the ligand escaping the binding pocket at various times throughout the simulations (Suppl. Fig. S2A). Calculating the average minimum distance between ligand and protein over the simulation periods (Suppl. Fig. S3) sheds light on the situation, revealing that the ligand from the hydroxychloroquine-H655Y system is moving away from the protein binding pocket at around 13 ns, while in the case of other ligands, the ligands continue to bind at their respective binding pockets. There is a substantial alteration in protein structure across the simulation times in all systems. Using trajectories from molecular dynamics simulations, principal component analysis (PCA) was

used to analyze changes in protein structure. To calculate the number of conformational changes, we first generated eigenvalues by diagonalizing the covariance matrix of C α atomic fluctuations against the equivalent eigenvector (EV) indices. Figure 5v shows that the ivermectin B1a-T478K and remdesivir-H655Y systems have a larger subspace, and (Fig. 5vi) shows that their eigenvalue is greater. This strongly suggests that C α atoms of proteins in these two systems undergo significant conformational changes. However, Ivermectin B1b-T478K exhibits less C α -atom motion and occupies a smaller subspace with a lower eigenvalue. It clearly indicates stability of the system in comparison to other. If we will observe other MD parameters for this complex, then this system is quite stable and has better MD parameters in comparison to other. For all systems, we have additionally quantified the number of H-bonds between the ligand and the proteins (Fig. 5vii). Hydroxychloroquine-H655Y, ivermectin B1a-T478K, molnupiravir-H655Y, remdesivir-H655Y, and ivermectin B1b-T478K all had an average of zero, one, two, one, and one H-bonds, respectively. The MM-PBSA binding free energy for each system has been determined and is depicted in (Fig. 5viii). Ivermectin B1b-T478K has the highest binding free energy, at 88.5 kilojoules per mole, followed by remdesivir-H655Y (-76 kJ/mol), ivermectin B1a-T478K (-70.9 kJ/mol), molnupiravir-H655Y (-35.8 kJ/mol), and hydroxychloroquine-H655Y (6.3 kJ/mol). Table 4 lists all the systems and their respective binding free energy contributions, including van der Waals, electrostatic, polar solvation, and SASA energies. In light of these findings, it is apparent that the ivermectin B1b-T478K system is the most stable. Collecting all these pieces of evidence, the efficacy of ivermectin and remdesivir have the highest efficacy in binding and interacting with the most virulent strain of the omicron variant of SARS-CoV-2. The schematic representation of the total flow of work is depicted in (Fig. 6).

Table 4 — The binding energy of the docked complexes (in kJ/mol)

Energy (in kJ/mol)	Hydroxychloroquine-H655Y	Ivermectin B1a-T478K	Molnupiravir-H655Y	Remdesivir-H655Y	Ivermectin B1b-T478K
van der Waals	-9.3 \pm 2.8	-138.4 \pm 3.3	-87.8 \pm 3	-170.4 \pm 2.6	-177.1 \pm 7.1
Electrostatic	-2.3 \pm 0.8	-23.7 \pm 1.7	-30.5 \pm 2.7	-27.8 \pm 2.1	-48.6 \pm 4
Polar solvation	18.8 \pm 0.02	109.6 \pm 3.6	94.3 \pm 3.4	142.8 \pm 3.8	158.7 \pm 8.3
SASA	-1.3 \pm 0.4	-18.4 \pm 0.4	-11.9 \pm 0.2	-20.6 \pm 0.2	-21 \pm 0.7
Binding free energy	6.3 \pm 0.6	-70.9 \pm 2.6	-35.8 \pm 2.1	-76 \pm 1.9	-88.5 \pm 5.2

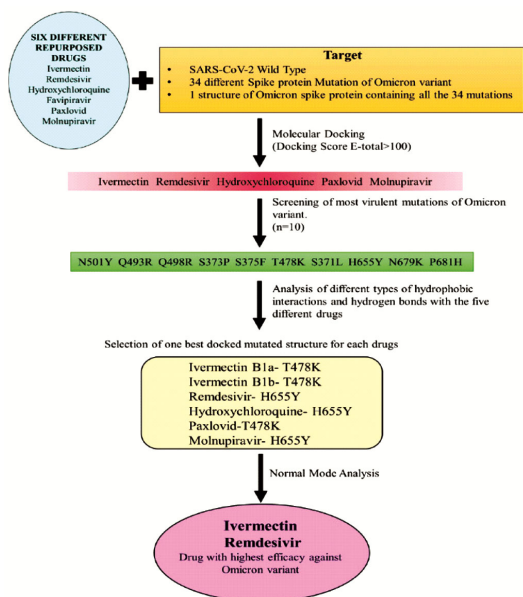


Fig. 6 — Schematic representation of the experimental design and results

Conclusion

The scientific communities are currently primarily interested in creating a potent treatment against the most virulent strain of COVID-19. In this study, the principal pathogenic proteins of the various virulent mutants of the omicron variant of SARS-CoV-2 and their spike protein were analyzed to determine the binding efficacy with ivermectin and other promising FDA-approved repurposed drugs. Among the six different drugs selected in this study, *viz.*, ivermectin, remdesivir, hydroxychloroquine, favipiravir, paxlovid, and molnupiravir, the docking score of ivermectin, remdesivir, hydroxychloroquine, paxlovid, and molnupiravir shows significant binding. Among the different mutants of the omicron variant, we have further selected the top 10 most virulent and concerning mutants of omicron. The docking of these top 10 highly mutated strains and the five repurposed drugs shows both homolog of ivermectin and paxlovid had greater binding efficiency to mutant protein T478K whereas, remdesivir, hydroxyl-chloroquine, and molnupiravir had binding efficiency to mutant protein H655Y.

The binding free energy of ivermectin with the Omicron variant spike protein was calculated to be -88.5 kcal/mol, indicating a strong binding affinity. Additionally, molecular dynamics simulations showed a stable interaction over a 50 ns simulation with an RMSD of less than 2.5 Å, suggesting a robust and persistent binding mode. Collectively, these suggest that both ivermectin and remdesivir can be used as

repurposed drugs against the treatment of the omicron variant of SARS-CoV-2. Although the docking and molecular dynamics simulations indicate that ivermectin and remdesivir have potential as treatments against the Omicron variant, these findings must be validated through in-vitro and in-vivo studies.

Acknowledgement

RP acknowledges DST-SERB for the award of Junior Research Fellowship (JRF). SM thanks Department of Science and Technology- Science and Engineering Research Board (DST-SERB) (Ref no.: CRG/2021/002605), Government of India for providing financial support and grants for research. Assistance of former research scholar of IBIL Ms. Somrita Padma is acknowledged.

Conflict of interest

All authors declare no conflict of interest.

References

- 1 WHO, Coronavirus 2023. WHO Coronavirus (COVID-19). (2023) <https://covid19.who.int/> (accessed on 25 Jul2023).
- 2 Tian D, Sun Y & Xu H, Ye Q, The emergence and epidemic characteristics of the highly mutated SARS-CoV-2 Omicron variant. *J Med Virol*, 94 (2022)2376.
- 3 Patra R, Das NC & Mukherjee S, Toll-Like Receptors (TLRs) as Therapeutic Targets for Treating SARS-CoV-2: An Immunobiological Perspective BT - Coronavirus Therapeutics – Volume I: Basic Science and Therapy Development. In: Asea AAA, Kaur P (eds). *Springer International Publishing: Cham*, (2021) 87.
- 4 Das NC, Chakraborty P, Bayry J & Mukherjee S, Comparative binding ability of human monoclonal antibodies against omicron variants of SARS-CoV-2: An *In silico* investigation. *Antibodies*, 12 (2023) 17.
- 5 Choudhury A, Mukherjee G & Mukherjee S, Chemotherapy vs. Immunotherapy in combating COVID19: An update. *Hum. Immunol*, 82 (2021) 649.
- 6 Choudhury A & Mukherjee S, *In silico* studies on the comparative characterization of the interactions of SARS-CoV-2 spike glycoprotein with ACE-2 receptor homologs and human TLRs. *J Med Virol*, 92 (2020) 2105.
- 7 Patra R, Das NC, Bhattacharya M, Shit PK, Patra BC & Mukherjee S, Applications of Artificial Intelligence (AI) Protecting from COVID-19 Pandemic: A Clinical and Socioeconomic Perspective BT - Computational Intelligence Techniques for Combating COVID-19. In: Kautish S, Peng SL, Obaid AJ (eds). *Springer International Publishing: Cham*,(2021) 45.
- 8 Sabir DK, Analysis of SARS-COV2 spike protein variants among Iraqi isolates. *Gene reports*, 26 (2022) 101420.
- 9 Mertens J, Coppens J, Loens K, Le Mercier M, Xavier BB, Lammens C, Vandamme S, Jansens H, Goossens H & Matheeußen V, Monitoring the SARS-CoV-2 pandemic: screening algorithm with single nucleotide polymorphism detection for the rapid identification of established and emerging variants. *Clin Microbiol Infect Off Publ Eur Soc Clin Microbiol Infect Dis*, 28 (2022) 124.

- 10 Shah VK, Fimal P, Alam A, Ganguly D & Chattopadhyay S, Overview of Immune response during SARS-CoV-2 infection: lessons from the past. *Front Immunol*, 11 (2020) 1949.
- 11 Das NC, Chakraborty P, Bayry J & Mukherjee S, *In silico* analyses on the comparative potential of therapeutic human monoclonal antibodies against newly emerged SARS-CoV-2 variants bearing mutant spike protein. *Front Immunol*, 12 (2022) 782506.
- 12 Patra R, Chandra Das N & Mukherjee S, Targeting human TLRs to combat COVID-19: A solution? *J Med Virol*, 93 (2021) 615.
- 13 Gupta Y, Savytskyi OV, Coban M, Venugopal A, Pleqi V, Weber CA, Chitale R, Durvasula R, Hopkins C, Kempaiah P & Caulfield TR, Protein structure-based *in silico* approaches to drug discovery: Guide to COVID-19 therapeutics. *Mol Aspects Med*, 91 (2023) 101151.
- 14 Choudhury A, Das NC, Patra R & Mukherjee S, *In silico* analyses on the comparative sensing of SARS-CoV-2 mRNA by the intracellular TLRs of humans. *J Med Virol*, 93 (2021) 2476.
- 15 Das CN, Labala KR, Patra R, Chatteraj A & Mukherjee S, *In silico* Identification of new anti-sars-cov-2 agents from bioactive phytocompounds targeting the viral spike glycoprotein and human TLR4. *Lett Drug Des Discov*, 19 (2022) 175.
- 16 Kalamatianos KG, *In silico* drug repurposing for coronavirus (COVID-19): screening known HCV drugs against the SARS-CoV-2 spike protein bound to angiotensin-converting enzyme 2 (ACE2) (6M0J). *Mol Divers*, 27 (2023) 1087.
- 17 Aminpour M, Cannariato M, Preto J, Safaeeardebili ME, Moracchiato A, Doria D, Donato F, Zizzi EA, Deriu MA, Scheim DE & Santin AD, *In silico* analysis of the multi-targeted mode of action of ivermectin and related compounds. *Computation*, 10 (2022) 51.
- 18 Alam S, Kamal TB, Sarker MMR, Zhou J-R, Rahman SMA & Mohamed IN, Therapeutic Effectiveness and Safety of Repurposing Drugs for the Treatment of COVID-19: Position Standing in 2021. *Front Pharmacol*, 12 (2021) 659577.
- 19 Fiolet T, Guihur A, Rebeaud ME, Mulot M, Peiffer-Smadja N & Mahamat-Saleh Y, Effect of hydroxychloroquine with or without azithromycin on the mortality of coronavirus disease 2019 (COVID-19) patients: a systematic review and meta-analysis. *Clin Microbiol Infect*, 27 (2021) 19.
- 20 Patra R, Bhattacharya M & Mukherjee S, IoT-Based Computational Frameworks in Disease Prediction and Healthcare Management: Strategies, Challenges, and Potential BT - IoT in Healthcare and Ambient Assisted Living. In: Marques G, Bhoi AK, Albuquerque VHC de, K.S. H (eds). Springer Singapore: Singapore, 2021, pp 17.
- 21 Choudhury A, Das NC, Patra R, Bhattacharya M, Ghosh P, Patra BC & Mukherjee S, Exploring the binding efficacy of ivermectin against the key proteins of SARS-CoV-2 pathogenesis: an *In silico* approach. *Future Virol*, 16 (2021) 277.
- 22 Araf Y, Akter F, Tang YD, Fatemi R, Parvez MS, Zheng C & Hossain MG, Omicron variant of SARS-CoV-2: Genomics, transmissibility, and responses to current COVID-19 vaccines. *J Med Virol*, 94 (2022) 1825.
- 23 Macindoe G, Mavridis L, Venkatraman V, Devignes MD & Ritchie DW, HexServer: an FFT-based protein docking server powered by graphics processors. *Nucleic Acids Res*, 38 (2010) W445.
- 24 Salentin S, Schreiber S, Haupt VJ, Adasme MF & Schroeder M, PLIP: fully automated protein-ligand interaction profiler. *Nucleic Acids Res*, 43 (2015) W443.
- 25 Tiwari SP, Fuglebakk E, Hollup SM, Skjærven L, Cragnolini T & Grindhaug SH, WEBnm@ v2.0: Web server and services for comparing protein flexibility. *BMC Bioinformatics*, 15 (2014) 427.
- 26 Padma S, Patra R, Sen Gupta PS, Panda SK, Rana MK & Mukherjee S, Cell surface fibroblast activation protein-2 (Fap2) of *Fusobacterium nucleatum* as a vaccine candidate for therapeutic intervention of human colorectal cancer: an immunoinformatics approach. *Vaccines*, 11 (2023) 525.
- 27 Sen Gupta PS, Biswal S, Panda SK, Ray AK & Rana MK, Binding mechanism and structural insights into the identified protein target of COVID-19 and importin- α with *in vitro* effective drug ivermectin. *J Biomol Struct Dyn*, 40 (2022) 2217.
- 28 Sen Gupta PS, Panda SK, Nayak AK & Rana MK, Identification and Investigation of a Cryptic Binding Pocket of the P37 Envelope Protein of Monkeypox Virus by Molecular Dynamics Simulations. *J Phys Chem Lett*, 14(2023) 3230.
- 29 Hornak V, Abel R & Okur A, Strockbine B, Roitberg A, Simmerling C. Comparison of multiple Amber force fields and development of improved protein backbone parameters. *Proteins*, 65 (2006) 712.
- 30 Panda SK, Saxena S, Gupta PS Sen & Rana MK, Inhibitors of Plasmepsin X Plasmodium falciparum: Structure-based pharmacophore generation and molecular dynamics simulation. *J Mol Liq*, 340 (2021) 116851.
- 31 Malin JJ, Suárez I, Priesner V, Fätkenheuer G & Rybniker J, Remdesivir against COVID-19 and Other Viral Diseases. *Clin Microbiol Rev*, 34 (2020) e00162.
- 32 Eweas AF, Alhossary AA & Abdel-Moneim AS, Molecular docking reveals ivermectin and remdesivir as potential repurposed drugs against SARS-CoV-2. *Front Microbiol*, 11 (2021) 592908.
- 33 Fox RI, Mechanism of action of hydroxychloroquine as an antirheumatic drug. *Semin Arthritis Rheum*, 23 (1993) 82.
- 34 Agrawal U, Raju R & Udwadia ZF, Favipiravir: A new and emerging antiviral option in COVID-19. *Med J Armed Forces India*, 76 (2020) 370.
- 35 Rosenke K, Okumura A, Lewis MC, Feldmann F, Meade-White K, Bohler WF, Griffin A, Rosenke R, Shaia C, Jarvis MA & Feldmann H, Molnupiravir (MK-4482) is efficacious against Omicron and other SARS-CoV-2 variants in the Syrian hamster COVID-19 model. *bioRxiv Prepr Serv Biol*, (2022).
- 36 Du X, Li Y, Xia YL, Ai SM, Liang J, Sang P, Ji XL & Liu SQ, Insights into Protein-Ligand Interactions: Mechanisms, Models, and Methods. *Int J Mol Sci*, 17 (2016) 144.
- 37 Szczepanski MJ, Czystowska M, Szajnik M, Harasymczuk M, Boyiadzis M & Kruk-Zagajewska A, Triggering of Toll-like receptor 4 expressed on human head and neck squamous cell carcinoma promotes tumor development and protects the tumor from immune attack. *Cancer Res*, 69 (2009) 3105.
- 38 Zhou HX & Pang X, Electrostatic Interactions in Protein Structure, Folding, Binding, and Condensation. *Chem Rev*, 118 (2018) 1691.